Two-channel anomalous Hall effect originating from the intermixing in Mn_2CoAl/Pd thin films

Yao Zhang [1,2,3] and Simon Granville [1,2,*]

[1] *Robinson Research Institute, Victoria University of Wellington, Wellington, New Zealand*
[2] *MacDiarmid Institute for Advanced Materials and Nanotechnology, Wellington, New Zealand*
[3] *School of Chemical and Physical Sciences, Victoria University of Wellington, Wellington, New Zealand*

(Received 11 September 2022; accepted 4 October 2022; published 12 October 2022)

The anomalous Hall effect (AHE) is an electronic transport phenomenon with rich physics. In thin magnetic films and multilayers, an unusual peak observed in AHE is often identified as the topological Hall effect (THE), induced by topologically nontrivial spin textures. However, it is a challenge to determine whether this unusual peak truly originates from such spin textures or is an artifact due to inhomogeneities. In this work, we systematically study the Pd thickness and temperature dependence of the Hall effect in Mn_2CoAl/Pd thin films. We observe an unusual peak in the Pd thickness dependence and rule out that the origin of the peak is from the topologically nontrivial spin textures by directly imaging the magnetic domain structures. We also build a model for the AHE based on the sum of contributions from Mn_2CoAl and an intermixed CoPd alloy. These materials have opposite signs of the AHE and different coercive fields, which successfully explains the thickness and temperature behaviors of the unusual peak. Our results show that the interface mixing layer can play an important role in the interpretation of the AHE in ferromagnet/heavy metal systems.

DOI: 10.1103/PhysRevB.106.144414

I. INTRODUCTION

Topologically nontrivial spin textures with chirality and emergent phenomena create opportunities to design energy efficient and miniaturized spintronics devices [1,2]. Among these spin textures, magnetic skyrmions are quasiparticles with noncollinear spin configuration and nanoscale dimension enabling them to be used as information carriers [3,4]. They have been observed in single crystals with a noncentrosymmetric lattice [5,6] and in ferromagnet-heavy metal ultrathin films or multilayers [7,8].

Due to the topologically nontrivial property of the magnetic skyrmions, an emergent magnetic field can be induced. The moving electrons will be scattered by this magnetic field and thus give rise to a transverse resistance, the so-called topological Hall effect (THE) [9,10]. With the contribution of THE, the total Hall resistance of ferromagnetic materials with magnetic skyrmions can be given as $R_{xy} = R_{OHE} + R_{AHE} + R_{THE}$, where R_{OHE} and R_{AHE} are the ordinary Hall effect and the anomalous Hall effect (AHE), respectively. The magnitude of R_{THE} is generally proportional to the density of the skyrmions [10,11]. Thus, for the Hall effect measurement of the magnetic skyrmion host materials, an unusual peak or hump appearing near the coercive field has been often attributed to THE. The observation of this unusual peak has been used as an electrical signature to verify the presence of skyrmions in various thin film systems [12–15].

However, the origins of this unusual peak have been debated recently, and an alternative interpretation related to the superposition of two anomalous Hall channels has been proposed [16]. For instance, an unusual peak was observed in the single layer $SrRuO_3$ ultrathin films, which can be explained by the conventional inhomogeneity of the coercive field and thickness with the opposite sign of AHE [17–19]. This unusual peak can also be induced by the compositional inhomogeneity in rare-earth transition-metal ferrimagnetic alloys, *e.g.*, the Co_xGd_{1-x} alloy thin films in which Co and Gd show opposite sign of AHE [20]. Several reviews have recently appeared that summarize experimental observations of this peak in various materials as well as its potential origins [21–23].

In ferromagnet-heavy metal multilayers, it is well known that the Dzyaloshinskii-Moriya interaction (DMI) can be induced at the interface between the ferromagnetic layer and the heavy metal layer due to the broken inversion symmetry and strong spin-orbit coupling [24,25]. Because DMI favoring noncollinear spin states competes with the exchange and magnetic anisotropy interactions favoring collinear spin states, the magnetic skyrmions can be stabilized as a ground state in the multilayer systems [8]. Therefore, the unusual peak observed in these systems is usually ascribed to THE [13,26]. However, Gerber proposed that in $[Co/Pd]_n$ multilayers (where n corresponds to the number of repetition), an intermixing layer at the interface exhibits opposite sign of AHE compared with the ferromagnetic layer, and thus gives rise to an unusual peak [27]. Yet, in the multilayers, the interfaces are complicated, making it hard to quantitatively identify the relationship of the unusual peak and the intermixing layer. Also, still unknown is the influence of thickness of heavy metal on the unusual peak.

To investigate the origins of the unusual peak in ferromagnet-heavy metal ultrathin film systems, we have studied a simple trilayer system, $MgO/Mn_2CoAl/Pd$ thin film, where we only need to be concerned with one interface, between the Mn_2CoAl and Pd layer. We have observed an unusual peak in the Hall resistivity, which we previously

*simon.granville@vuw.ac.nz

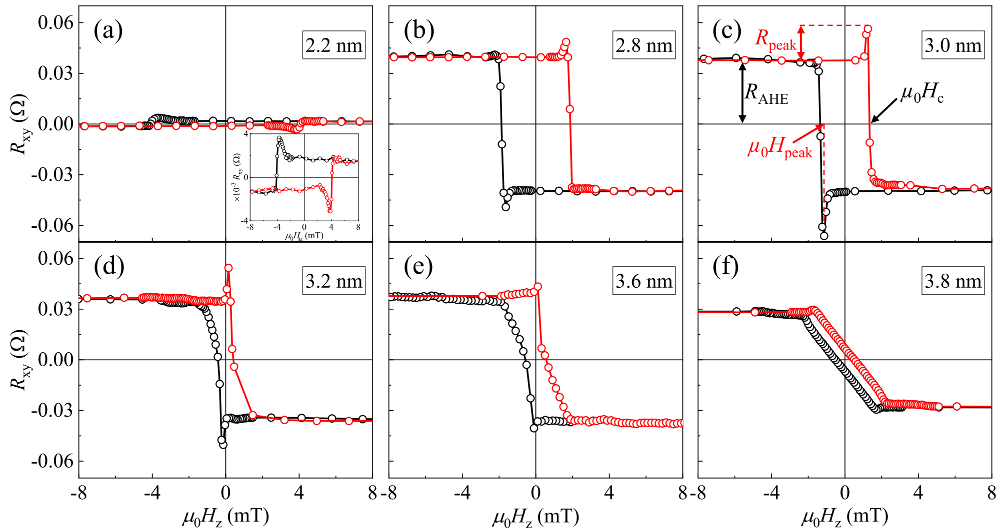

FIG. 1. The Hall effect for MgO(1.6 nm)/Mn_2CoAl(2.6 nm)/Pd(2.2–3.8 nm) trilayers at 300 K. The inset shows the zoomed in region of the loop. Black branch: positive-to-negative magnetic field sweeping; red branch: negative-to-positive magnetic field sweeping.

identified as the topological Hall effect [13]. Furthermore, DMI is present and we have studied magnetic skyrmions in this system using magneto-optical Kerr effect microscopy [28,29]. Therefore, it is an ideal system to investigate the relation of the unusual peak and the magnetic skyrmions.

In this work, we prepared MgO/Mn_2CoAl/Pd trilayers with various thickness of Pd layer and investigated the Hall effect and magnetic domain structures. We observed an unusual peak in Hall effect and demonstrated that the origin is not from topologically nontrivial spin textures. The Pd thickness and temperature behaviors of the unusual peak can be clarified by a model based on two different magnetic materials with an opposite sign of AHE and difference of coercive field.

II. EXPERIMENTAL METHOD

A series of trilayers: MgO(1.6 nm)/Mn_2CoAl(2.6 nm)/Pd(2.2–4.4 nm) were deposited on thermally oxidized Si/SiO_2(300 nm) substrates by magnetron sputtering with a base pressure below 4×10^{-8} Torr. Samples were grown at ambient temperature while rotating the sample holder and then post-growth annealed *in situ* for 1 hour at 300. Our previous work has shown that samples prepared in this way demonstrate perpendicular magnetic anisotropy [28,30].

Magneto-optical Kerr effect (MOKE) measurements with a green light ($\lambda = 540$ nm) were used to obtain the hysteresis loops and the magnetic domain morphology at ambient temperature in differential imaging mode. An out-of-plane magnetic field was used and the magnetic domains imaged in polar mode, to detect the out-of-plane component of magnetization. The Hall resistance was measured in a Van der Pauw geometry by using the resistivity option of a Physical Property Measurement System (PPMS, Quantum Design).

III. RESULTS

A. Pd thickness dependence of the unusual AHE

The Hall effect of MgO(1.6 nm)/Mn_2CoAl(2.6 nm)/Pd (t_{Pd} nm) thin films was performed at 300 K, as shown in Fig. 1. In our system, R_{OHE} is much smaller than R_{AHE} and can be neglected at the low magnetic fields of the measurements presented here. For the sample with thin Pd layer $t_{Pd} = 2.2$ nm it shows a positive AHE with a very small $R_{xy} = 0.0013$ Ω, as shown in the inset of Fig. 1(a). Upon sweeping the magnetic field from saturation, there is a small peak close to the coercive field μ_0H_c, present for both positive-to-negative and negative-to-positive field sweeps. By increasing t_{Pd}, the sign of AHE changes to negative with an obvious unusual peak, as shown in Figs. 1(b) and 1(c). We have previously identified this peak as the THE due to the existence of the topologically nontrivial spin textures. After $t_{Pd} \geqslant 3.2$ nm, the unusual peak starts to decrease, and almost disappears for the trilayers with a thick Pd layer, as shown in Figs. 1(d)–1(f).

The values of R_{AHE} and R_{peak} were extracted from the Hall effect measurements and plotted as a function of t_{Pd} (see Fig. 2), where R_{peak} is the magnitude of the peak defined as R_{peak}=R_{xy}-R_{OHE}-R_{AHE} [see Fig. 1(c)]. Figure 2(a) shows that the sign of R_{AHE} changes from positive to negative when $t_{Pd} = 2.4$ nm. The value of R_{AHE} increases to a maximum -0.040 Ω at $t_{Pd} = 2.8$ nm, and then decays to -0.025 Ω at $t_{Pd} = 4.4$ nm. For the case of R_{peak}, the value of R_{peak} increases from around 0 to a maximum 0.023 Ω in the range of $t_{Pd} = 2.2$ to 3.0 nm, and then drops to 0 in the range of $t_{Pd} = 3.2$ to 4.4 nm, as shown in Fig. 2(b).

B. Magnetic domain morphology

To answer whether this unusual peak is THE originating from the magnetic skyrmions or not, the magnetic domain structures of Mn_2CoAl trilayers have been characterized by MOKE. Figure 3 shows the typical hysteresis loops and the magnetic domain structures for the same films MgO(1.6 nm)/Mn_2CoAl(2.6 nm)/Pd(t nm) with an external out-of-plane magnetic field at ambient temperature. For the hysteresis loops, the coercive field decreases with raising t_{Pd} due to the reduction of the perpendicular magnetic anisotropy with thicker Pd layer. Especially for $t_{Pd} = 3.8$ nm, the remanent magnetization, magnetization at zero-field, is close to 0

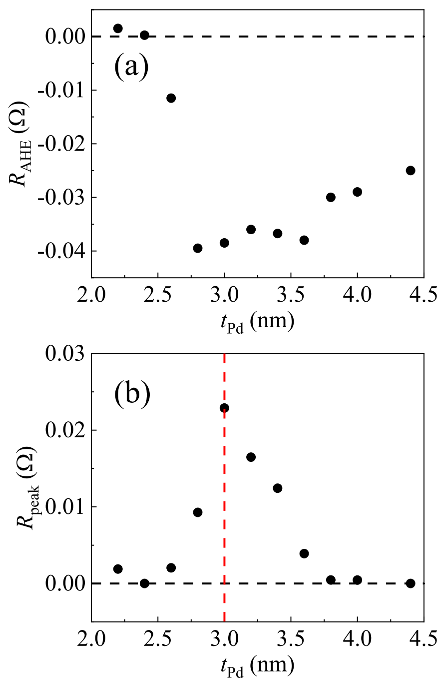

FIG. 2. R_{AHE} and R_{peak} as a function of the thickness of the Pd layer.

[see Fig. 3(m)] suggesting that this thin film shows a magnetic anisotropy closing to the spin-reorientation transition between the out-of-plane and in-plane directions. It should be noted that the coercive field measured by MOKE is larger than that of the Hall effect results. The reason is that the sweep rate of the magnetic field for electrical transport measurements is much slower than that of the MOKE measurements. The field stabilisation time for the electrical transport measurements in the PPMS is longer than it is for the MOKE equipment, and of a similar time as the nucleation time of the magnetic domains. Hence, in the Hall measurements the magnetic domains are indeed nucleated and propagated, and thus a relatively small magnetic field is needed to switch the magnetization compared with the MOKE measurement, which measures over faster timescales compared to the dynamic of magnetic domains.

Here, we will discuss the magnetic domain structures and the nucleation process for these Mn_2CoAl trilayers. Samples were magnetically saturated first with a large enough negative magnetic field, −18 mT. Then, magnetic domain images were taken continuously by MOKE while sweeping the field from negative to positive. For samples with $t_{Pd} = 2.2$ nm, one can see that a uniform magnetic domain nucleates at a defect position and then propagates with increasing the magnetic field as shown in Figs. 3(b)–3(d). For samples with $t_{Pd} = 3.0$ nm, which shows the highest unusual peak in the R_{xy}, several magnetic domains nucleate near the coercive field and then propagate with the rise of the magnetic field as shown in Figs. 3(f)–3(h). In Figs. 3(g) and 3(h), there are labyrinth structures visible within the larger area of black reversed magnetic domain. By increasing $t_{Pd} = 3.2$ nm, now

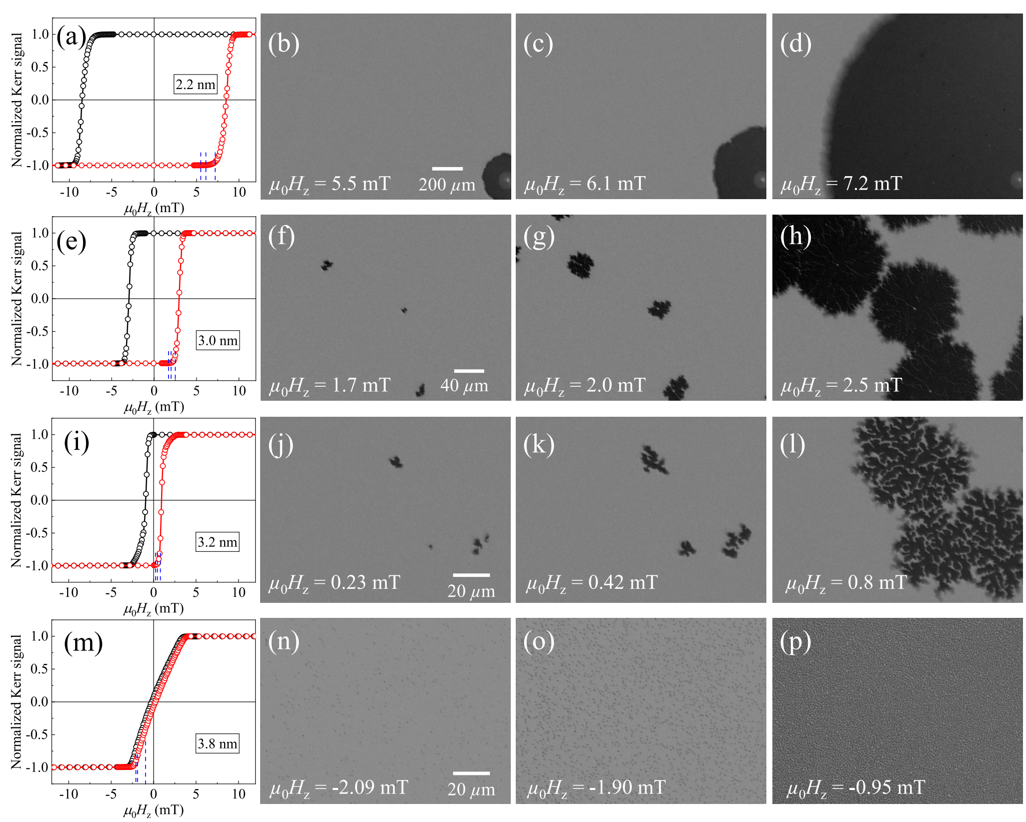

FIG. 3. The hysteresis loops and the corresponding magnetic domain images for MgO(1.6 nm)/Mn_2CoAl(2.6 nm)/Pd(2.2–3.8 nm) trilayers at ambient temperature. The blue dash lines show the magnetic field where the magnetic domain images were taken. Black branch: positive-to-negative magnetic field sweeping; red branch: negative-to-positive magnetic field sweeping.

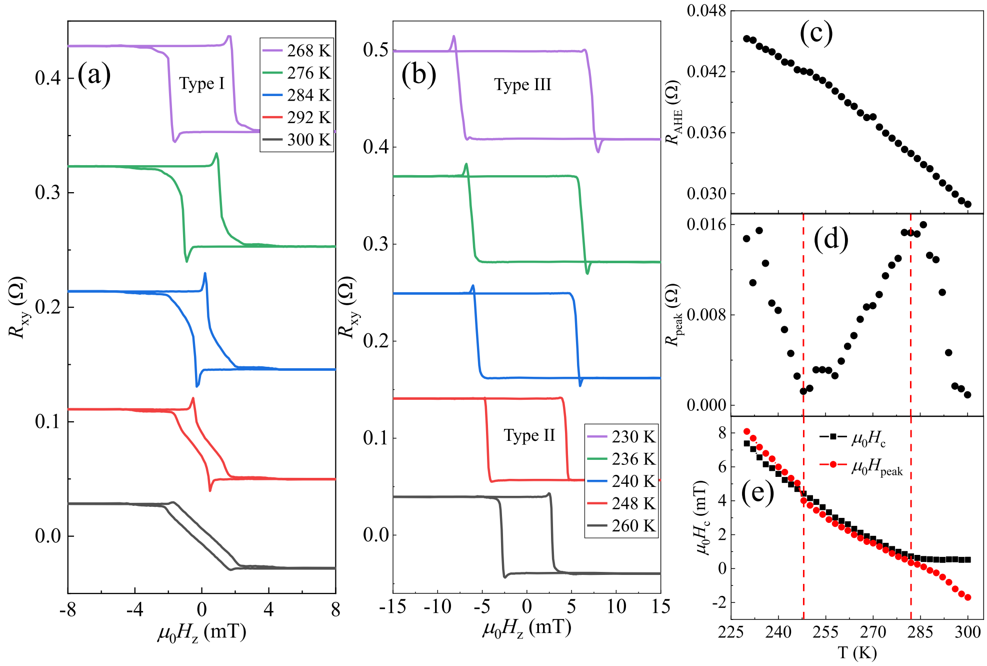

FIG. 4. (a)–(b) The temperature dependence of Hall effect for MgO(1.6 nm)/Mn_2CoAl(2.6 nm)/Pd(3.8 nm) trilayer measured from 300 K to 230 K. (c)–(e) R_{AHE}, R_{peak}, $\mu_0 H_c$ and $\mu_0 H_{\mathrm{peak}}$ as a function of the temperature, respectively.

reaching a regime where there is a relatively weak perpendicular magnetic anisotropy, more uniform magnetic domains transform to the labyrinth domains as shown in Figs. 3(j)–3(l). For samples with $t_{\mathrm{Pd}} = 3.8$ nm at the spin-reorientation transition regime, magnetic skyrmions with around 800 nm size nucleate as shown in Fig. 3(n) and established in our previous work [28,29]. The density of the magnetic skyrmions increases under a lower magnetic field as shown in Figs. 3(o) and 3(p).

It has been shown that there is an unusual peak observed in samples with $t_{\mathrm{Pd}} = 2.2$, 3.0, and 3.2 nm in Fig. 1. However, we only observe uniform magnetic domains and labyrinth domains in those samples. Though the labyrinth domains may show chirality with noncollinear domain walls due to the interfacial DMI in these films, there should exhibit two peaks in each branch when sweeping the field down from saturation, where a peak happens at the nucleation regime and another peak with opposite sign should appear at the annihilation regime where some unreversed labyrinth domains remain (see Supplemental Materials [31]) [32]. Here, only one peak is observed at each branch suggesting that the unusual peak is not related to the chiral labyrinth domains.

Kan *et al.* reported that the value of the THE resistance should depend on the sweep rate of magnetic field [17]. In the Supplementary Materials [31], the Hall effect measurements with different magnetic field sweep rate have been presented. One can see that R_{peak} is independent of the sweep rate while both $\mu_0 H_c$ and $\mu_0 H_{\mathrm{peak}}$ change, where $\mu_0 H_{\mathrm{peak}}$ corresponds to the magnetic field of the peak. In Ref. [17], this sweep rate behavior can be understood in the conventional magnetization reversal process rather than the topologically noncollinear spin textures. Furthermore, we notice that a large amount of magnetic skyrmions have been observed in the sample with $t_{\mathrm{Pd}} = 3.8$ nm, where only a very weak R_{xy} peak is obtained. This sample also only shows one peak at each branch. Previous studies reported that magnetic skyrmions in ultrathin films cause a very weak THE, only 10% of R_{AHE}, in which a peak cannot be directly observed but obtained by scaling the difference of the AHE and magnetization loops [11,33]. It is hard to believe that, in the sample with $t_{\mathrm{Pd}} = 3.0$ nm, R_{peak} with a size of 57% of R_{AHE} results from the topologically noncollinear spin textures. Based on the above discussion, we conclude that the peak does not originate from the topologically noncollinear spin textures.

C. Temperature dependence of the unusual AHE

To find out the origin of the unusual peak, the temperature dependence of Hall measurements for MgO(1.6 nm)/Mn_2CoAl(2.6 nm)/Pd(3.8 nm) trilayer has been performed from 300 K to 230 K as shown in Fig. 4. By cooling down the temperature, $\mu_0 H_c$ of the hysteresis loops becomes larger and the remanent magnetization equals the saturation magnetization, indicating that the perpendicular magnetic anisotropy becomes strong at low temperature as shown in Figs. 4(a)–4(b). One can observe three types of hysteresis loops: loops with a peak $\mu_0 H_c \geqslant \mu_0 H_{\mathrm{peak}}$ (Type I), loops without a peak (Type II), and loops with a peak $\mu_0 H_c \leqslant \mu_0 H_{\mathrm{peak}}$ (Type III).

R_{AHE}, R_{peak}, $\mu_0 H_c$ and $\mu_0 H_{\mathrm{peak}}$ were extracted from the temperature-dependent Hall effect measurements, as shown in Figs. 4(c)–4(e), respectively. R_{AHE} increases linearly from 0.029 Ω to 0.045 Ω on cooling [see Fig. 4(c)]. Regarding R_{peak}, the temperature dependent behavior is relatively complicated and exhibits three regimes [see Fig. 4(d)]: R_{peak} increases from nearly 0 to maximum 0.015 Ω in the range

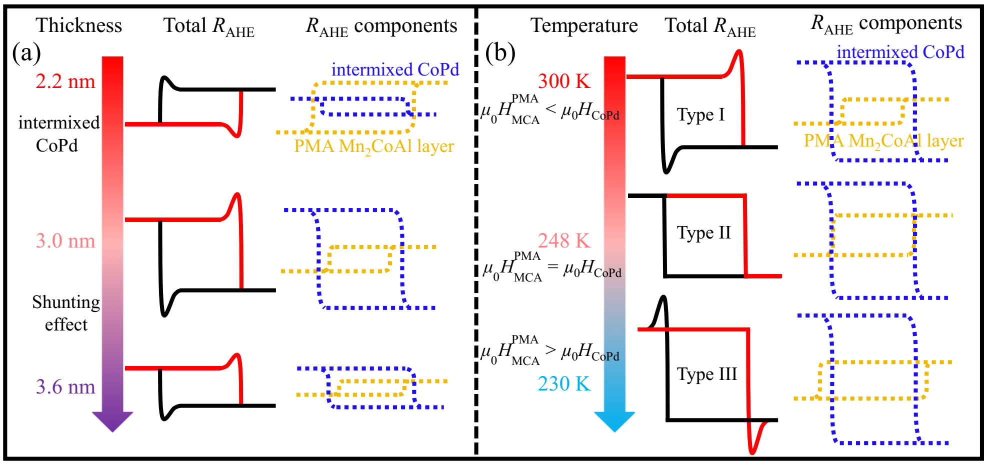

FIG. 5. The schematic of the model based on two magnetic contributions. The total R_{AHE} in a trilayer is a sum of two components: MCA layer and intermixed CoPd layer. (a) Model for Pd thickness dependent of AHE. (b) Model for temperature dependent of AHE. Black branch: positive-to-negative magnetic field sweeping; red branch: negative-to-positive magnetic field sweeping.

from 300 K to 282 K, then reduces to a minimum at 248 K, and finally increases to 0.015 Ω again at 230 K. In Fig. 4(e), $\mu_0 H_c$ and $\mu_0 H_{peak}$ were plotted together. In the range from 300 K to 282 K, $\mu_0 H_{peak}$ is less than $\mu_0 H_c$ while the difference between them becomes small on cooling. $\mu_0 H_{peak}$ approaches $\mu_0 H_c$ at 284 K and keeps a very small difference with $\mu_0 H_c$ until the temperature decreases to 248 K. After that, $\mu_0 H_{peak}$ is greater than $\mu_0 H_c$ in the range from 246 K to 230 K. Strikingly, the temperature-dependent relationship of $\mu_0 H_c$ and $\mu_0 H_{peak}$ shows completely the same three temperature regimes as the temperature behavior of R_{peak}, strongly suggesting that the magnitude of R_{peak} relates to the difference of $\mu_0 H_c$ and $\mu_0 H_{peak}$. Therefore, we think the unusual peak may result from two different magnetic species with opposite signs of AHE and different coercive fields.

D. Model based on two magnetic contributions

From our previous work, the ferromagnetic Mn_2CoAl layer shows a positive AHE from 300 K to 5 K [34]. Recently, Basha *et al.*, directly observed that there is an intermixing CoPd alloy in Co_2MnSi/Pd ultrathin films similar to our system [35]. Also, it is known that the CoPd alloy with excess Pd shows a negative AHE [36]. Thus, we establish a model based on Mn_2CoAl and intermixed CoPd alloy with opposite signs of AHE and different coercive fields to clarify the thickness and temperature dependence of the unusual peak.

We first discuss the relationship of the unusual peak and the Pd thickness. The schematic loops for the Pd thickness dependent AHE and unusual peak are summarised in Fig. 5(a). For the sample with a thin Pd layer, t_{Pd} = 2.2 nm, a small amount of intermixing at the Mn_2CoAl/Pd interface forms a CoPd alloy and contributes a weak negative AHE. The total measured AHE is dominated by the perpendicular magnetized Mn_2CoAl layer in this situation. If the coercive field of the intermixed CoPd alloy ($\mu_0 H_{CoPd}$) is less than the coercive field of perpendicular magnetized Mn_2CoAl ($\mu_0 H_{MCA}^{PMA}$), the total AHE is positive and a small peak can be observed [see Fig. 1(a)]. With increasing the thickness of the Pd layer, there is more CoPd formed with a stronger negative AHE and $\mu_0 H_{CoPd}$ increases so that the total AHE reverses to negative with a peak. Regarding the samples with a thick Pd layer, like $t_{Pd} \geqslant 3.2$ nm, most of the electric current will pass through the Pd layer because the bulk resistivity of Pd, ~11 μΩ cm [37], is much lower than that of Mn_2CoAl, 200 μΩ cm [34], which is the so-called shunting effect. This effect leads to a reduction of the net AHE of the Mn_2CoAl/Pd bilayer with intermixed CoPd at the interface and a decline of the peak for the samples with a thick Pd layer as shown in Fig. 2(b).

The temperature dependence of R_{peak} with three types of hysteresis loops can be also understood by this model. First, the total AHE stays negative for the thin film with $t_{Pd} = 3.8$ nm in the range from 300 K to 230 K as the intermixed CoPd alloy is the dominant contribution. Then, the transformation of hysteresis loops can be explained by the difference of $\mu_0 H_{MCA}^{PMA}$ and $\mu_0 H_{CoPd}$ illustrated in Fig. 5(b). In the range from 300 K to 250 K, the sample shows the Type I loops because $\mu_0 H_{MCA}^{PMA}$ is smaller than $\mu_0 H_{CoPd}$. For the magnitude of the peak, as the difference of the coercive field for both magnetic contributors is large enough to disentangle the value of AHE, R_{peak} only represents the component of intermixed CoPd alloy. By cooling down the temperature, the AHE of the CoPd will be increased which has been observed in the range from 300 K to 282 K in Fig. 4(e). However, in the range from 282 K to 248 K, $\mu_0 H_{CoPd}$ closes to $\mu_0 H_{MCA}^{PMA}$, meaning that the switch of the magnetization for both Mn_2CoAl and CoPd merges at the same field so that the peak decreases and disappears at 248 K, where $\mu_0 H_{CoPd}$ equals to $\mu_0 H_{MCA}^{PMA}$. By continuing to decrease the temperature, $\mu_0 H_{CoPd}$ starts to become greater than $\mu_0 H_{MCA}^{PMA}$, so that the switch of magnetization for both contributors again disentangles, and a peak can be observed again [see Fig. 4(e)].

IV. DISCUSSION

The temperature dependence of the coercive field can be described by a Sharrock-type formula [38],

$$\mu_0 H_c = \mu_0 H_0 \left[1 - \frac{kT}{E_0} \ln (f_0 t) \right], \tag{1}$$

where $\mu_0 H_0$ is the intrinsic coercive field at 0 K and E_0 is the zero-field energy barrier. $\ln(f_0 t)$ is an extrinsic term that relates to the sweeping field rate which is independent of temperature. Brown *et al.* reported $\mu_0 H_0 \sim M_s^{1.5}$ while E_0 is almost temperature insensitive in Co/Pd mutilayers [38], where M_s is the saturation magnetization. Given that M_s of perpendicular magnetized Mn_2CoAl trilayer (315 emu/cm^3 [28]) is larger than that of CoPd alloy which is Pd-rich (less than 200 emu/cm^3 [39]), we think $\mu_0 H_0$ of Mn_2CoAl is larger than that of CoPd alloy. Thus, the temperature dependence of coercive field of perpendicular magnetized Mn_2CoAl is more sensitive than CoPd alloy.

It has been reported that inhomogeneities could be the origin of the unusual peak in perovskite oxide thin films, like $SrRuO_3$ [18,19]. For this type of material, the sign of the AHE is determined by the intrinsic electronic structure and is sensitive to the thickness [40]. For instance, in single layer $SrRuO_3$ ultrathin films, the sign of AHE changes from negative to positive when decreasing thickness from 5 to 4 unit cells, so that an unusual peak for the films can be observed with thickness between 4 and 5 unit cells. Corresponding to the magnetic domains in this nonuniform thin film, a two-step magnetic switching behavior has been observed due to the mixture of magnetic domains for the area with a thickness variation [19]. In our films, we do see the mixture of the labyrinth domains and uniform magnetic domains, but this depends on the competition of the magnetic anisotropy, exchange interaction, and DMI rather than the thickness inhomogeneity of the Mn_2CoAl layer [8,28]. More importantly, unlike AHE in $SrRuO_3$, which is sensitive to the thickness or composition, the Mn_2CoAl layer is only known to show positive AHE [30,41,42]. Therefore, we think that the thickness inhomogeneity is not the origin in our system. Considering the interface between the Mn_2CoAl and Pd layers, it is reasonably assuming that an intermixed CoPd alloy can be formed at the interface and thus induce an unusual peak in AHE.

V. CONCLUSION

In summary, we fabricated Mn_2CoAl/Pd thin films with perpendicular magnetic anisotropy by varying the thickness of Pd layer in order to investigate the link between the observed Hall effect and the magnetic domains present. A THE-like peak was observed in the Hall effect hysteresis loops. By characterizing the magnetic domain morphology, we demonstrate that this unusual peak is not THE and rule out its origin as being topologically nontrivial spin textures. We believe that an intermixed CoPd alloy at the interface between the Mn_2CoAl and Pd layers plays a key role in the appearance of the unusual peak. A model based on Mn_2CoAl and intermixed CoPd alloy with opposite signs of AHE and different coercive fields fully explains the thickness and temperature-dependent behaviors of the unusual peak. For the Pd thickness dependence of the peak, the magnitude of the peak increases when increasing the thickness of Pd layer since there is more intermixed CoPd alloy formed. With thicker Pd layers, the reduction of the peak can be ascribed to the shunting effect through the low resistivity nonmagnetic Pd. For the temperature dependence of the peak, three types of AHE hysteresis loops can be observed due to the difference of the coercive field between the Mn_2CoAl and intermixed CoPd alloy.

ACKNOWLEDGMENTS

The MacDiarmid Institute is supported under the New Zealand Centres of Research Excellence Programme.

[1] S.-H. Yang, Spintronics on chiral objects, Appl. Phys. Lett. **116**, 120502 (2020).

[2] S.-H. Yang, R. Naaman, Y. Paltiel, and S. S. Parkin, Chiral spintronics, Nat. Rev. Phys. **3**, 328 (2021).

[3] A. Fert, N. Reyren, and V. Cros, Magnetic skyrmions: Advances in physics and potential applications, Nat. Rev. Mater. **2**, 17031 (2017).

[4] X. Zhang, Y. Zhou, K. M. Song, T.-E. Park, J. Xia, M. Ezawa, X. Liu, W. Zhao, G. Zhao, and S. Woo, Skyrmion-electronics: writing, deleting, reading and processing magnetic skyrmions toward spintronic applications, J. Phys.: Condens. Matter **32**, 143001 (2020).

[5] S. Mulbauer, B. Binz, F. Jonietz, C. Pfleiderer, A. Rosch, A. Neubauer, R. Georgii, and P. BoÌni, Skyrmion lattice in a chiral magnet, Science **323**, 915 (2009).

[6] X. Yu, Y. Onose, N. Kanazawa, J. H. Park, J. Han, Y. Matsui, N. Nagaosa, and Y. Tokura, Real-space observation of a two-dimensional skyrmion crystal, Nature (London) **465**, 901 (2010).

[7] S. Heinze, K. Von Bergmann, M. Menzel, J. Brede, A. Kubetzka, R. Wiesendanger, G. Bihlmayer, and S. Blügel, Spontaneous atomic-scale magnetic skyrmion lattice in two dimensions, Nat. Phys. **7**, 713 (2011).

[8] S. Woo, K. Litzius, B. Krüger, M.-Y. Im, L. Caretta, K. Richter, M. Mann, A. Krone, R. M. Reeve, M. Weigand *et al.*, Observation of room-temperature magnetic skyrmions and their current-driven dynamics in ultrathin metallic ferromagnets, Nat. Mater. **15**, 501 (2016).

[9] P. Bruno, V. K. Dugaev, and M. Taillefumier, Topological Hall Effect and Berry Phase in Magnetic Nanostructures, Phys. Rev. Lett. **93**, 096806 (2004).

[10] A. Neubauer, C. Pfleiderer, B. Binz, A. Rosch, R. Ritz, P. Niklowitz, and P. Böni, Topological Hall effect in the A phase of MnSi, Phys. Rev. Lett. **102**, 186602 (2009).

[11] M. Raju, A. Yagil, A. Soumyanarayanan, A. K. Tan, A. Almoalem, F. Ma, O. Auslaender, and C. Panagopoulos, The evolution of skyrmions in Ir/Fe/Co/Pt multilayers and their topological Hall signature, Nat. Commun. **10**, 696 (2019).

[12] J. Matsuno, N. Ogawa, K. Yasuda, F. Kagawa, W. Koshibae, N. Nagaosa, Y. Tokura, and M. Kawasaki, Interface-driven topological Hall effect in $SrRuO_3$-$SrIrO_3$ bilayer, Sci. Adv. **2**, e1600304 (2016).

[13] B. Ludbrook, G. Dubuis, A.-H. Puichaud, B. Ruck, and S. Granville, Nucleation and annihilation of skyrmions in Mn_2 CoAl observed through the topological Hall effect, Sci. Rep. **7**, 13620 (2017).

[14] J. C. Gallagher, K. Y. Meng, J. T. Brangham, H. L. Wang, B. D. Esser, D. W. McComb, and F. Y. Yang, Robust Zero-Field Skyrmion Formation in FeGe Epitaxial Thin Films, Phys. Rev. Lett. **118**, 027201 (2017).

[15] A. S. Ahmed, A. J. Lee, N. Bagués, B. A. McCullian, A. M. Thabt, A. Perrine, P.-K. Wu, J. R. Rowland, M. Randeria, P. C. Hammel *et al.*, Spin-Hall topological Hall effect in highly tunable Pt/ferrimagnetic-insulator bilayers, Nano Lett. **19**, 5683 (2019).

[16] D. Kan, T. Moriyama, K. Kobayashi, and Y. Shimakawa, Alternative to the topological interpretation of the transverse resistivity anomalies in $SrRuO_3$, Phys. Rev. B **98**, 180408(R) (2018).

[17] D. Kan, T. Moriyama, and Y. Shimakawa, Field-sweep-rate and time dependence of transverse resistivity anomalies in ultrathin $SrRuO_3$ films, Phys. Rev. B **101**, 014448 (2020).

[18] G. Kimbell, P. M. Sass, B. Woltjes, E. K. Ko, T. W. Noh, W. Wu, and J. W. Robinson, Two-channel anomalous Hall effect in $SrRuO_3$, Phys. Rev. Mater. **4**, 054414 (2020).

[19] L. Wang, Q. Feng, H. G. Lee, E. K. Ko, Q. Lu, and T. W. Noh, Controllable thickness inhomogeneity and Berry curvature engineering of anomalous Hall effect in $SrRuO_3$ ultrathin films, Nano Lett. **20**, 2468 (2020).

[20] T. Fu, S. Li, X. Feng, Y. Cui, J. Yao, B. Wang, J. Cao, Z. Shi, D. Xue, and X. Fan, Complex anomalous Hall effect of CoGd alloy near the magnetization compensation temperature, Phys. Rev. B **103**, 064432 (2021).

[21] G. Kimbell, C. Kim, W. Wu, M. Cuoco, and J. W. Robinson, Challenges in identifying chiral spin textures via the topological Hall effect, Commun. Mater. **3**, 1 (2022).

[22] X. Niu, B. Chen, N. Zhong, P.-H. Xiang, and C.-G. Duan, Topological Hall effect in $SrRuO_3$ thin films and heterostructures, J. Phys.: Condens. Matter **34**, 244001 (2022).

[23] H. L. Wang, Y. Dai, G. M. Chow, and J. Chen, Topological Hall transport: materials, mechanisms and potential applications, Prog. Mater. Sci. **130**, 100971 (2022).

[24] I. Dzyaloshinsky, A thermodynamic theory of "weak" ferromagnetism of antiferromagnetics, J. Phys. Chem. Solids **4**, 241 (1958).

[25] T. Moriya, Anisotropic superexchange interaction and weak ferromagnetism, Phys. Rev. **120**, 91 (1960).

[26] M. V. Sapozhnikov, N. S. Gusev, S. A. Gusev, D. A. Tatarskiy, Y. V. Petrov, A. G. Temiryazev, and A. A. Fraerman, Direct observation of topological Hall effect in Co/Pt nanostructured films, Phys. Rev. B **103**, 054429 (2021).

[27] A. Gerber, Interpretation of experimental evidence of the topological Hall effect, Phys. Rev. B **98**, 214440 (2018).

[28] Y. Zhang, G. Dubuis, T. Butler, and S. Granville, Fractal Analysis of Skyrmions Generated by Field-Assisted Fine-tuning of Magnetic Anisotropy, Phys. Rev. Appl. **15**, 014020 (2021).

[29] Y. Zhang, G. Dubuis, C. Doyle, T. Butler, and S. Granville, Nonvolatile and Volatile Skyrmion Generation Engineered by Ionic Liquid Gating in Ultrathin Films, Phys. Rev. Appl. **16**, 014030 (2021).

[30] Y. Zhang, G. Dubuis, T. Butler, S. Kaltenberg, E. Trewick, and S. Granville, Voltage-controlled switching of magnetic anisotropy in ambipolar Mn_2 CoAl/Pd bilayers, Phys. Rev. Appl. **17**, 034006 (2022).

[31] See Supplemental Material at http://link.aps.org/supplemental/10.1103/PhysRevB.106.144414 for details of the reverse process of labyrinth domains and magnetic field sweeping rate dependence of Hall effect.

[32] W. Wang, Y.-F. Zhao, F. Wang, M. W. Daniels, C.-Z. Chang, J. Zang, D. Xiao, and W. Wu, Chiral-bubble-induced topological Hall effect in ferromagnetic topological insulator heterostructures, Nano Lett. **21**, 1108 (2021).

[33] M. He, G. Li, Z. Zhu, Y. Zhang, L. Peng, R. Li, J. Li, H. Wei, T. Zhao, X.-G. Zhang *et al.*, Evolution of topological skyrmions across the spin reorientation transition in Pt/Co/Ta multilayers, Phys. Rev. B **97**, 174419 (2018).

[34] R. G. Buckley, T. Butler, C. Pot, N. M. Strickland, and S. Granville, Exploring disorder in the spin gapless semiconductor Mn_2 CoAl, Materials Research Express **6**, 106113 (2019).

[35] A. Basha, H. Fu, G. Levi, G. Leitus, A. Kovács, C. You, and A. Kohn, Interface alloying of ultra-thin sputter-deposited Co_2 MnSi films as a source of perpendicular magnetic anisotropy, J. Magn. Magn. Mater. **489**, 165367 (2019).

[36] S. Das, G. Kopnov, and A. Gerber, Detection of hydrogen by the extraordinary Hall effect in CoPd alloys, J. Appl. Phys. **124**, 104502 (2018).

[37] S. Shivaprasad, L. Udachan, and M. Angadi, Electrical resistivity of thin palladium films, Phys. Lett. A **78**, 187 (1980).

[38] C. S. Brown, J. Harrell, and S. Matsunuma, Time and temperature dependences of the magnetization reversal in a Co/Pd multilayer film, J. Appl. Phys. **100**, 053910 (2006).

[39] A. Bourezg and A. Kharmouche, Synthesis, structural and magnetic properties of Co_{100-x} Pd_x/GaAs thin films, Vacuum **155**, 612 (2018).

[40] D. J. Groenendijk, C. Autieri, T. C. van Thiel, W. Brzezicki, J. R. Hortensius, D. Afanasiev, N. Gauquelin, P. Barone, K. H. W. Van den Bos, S. van Aert, J. Verbeeck, A. Filippetti, S. Picozzi, M. Cuoco, A. D. Caviglia, Berry phase engineering at oxide interfaces, Phys. Rev. Res. **2**, 023404 (2020).

[41] G. Xu, Y. Du, X. Zhang, H. Zhang, E. Liu, W. Wang, and G. Wu, Magneto-transport properties of oriented Mn_2 CoAl films sputtered on thermally oxidized Si substrates, Appl. Phys. Lett. **104**, 242408 (2014).

[42] K. Kudo, A. Masago, S. Yamada, L. Kumara, H. Tajiri, Y. Sakuraba, K. Hono, and K. Hamaya, Positive linear magnetoresistance effect in disordered $L2_1$ B-type Mn_2 CoAl epitaxial films, Phys. Rev. B **103**, 104427 (2021).